

Visibility Estimation and Forecast in Foggy Weather

Shijie Yu, Kai You, Qiang Huang

Logistics Engineering College, Shanghai Maritime university, Shanghai 202010, China.

Abstract

Visibility is very important to highway driving safety. The main factors affecting visibility are fog and haze, and the formation and dissipation of fog has its own rules. Based on meteorological observation data and video data, the relationship between meteorological observation and visibility and the formation and dissipation of fog were estimated and predicted by establishing several models. First of all, through the establishment of multiple nonlinear regression model to analyze the impact of each meteorological element on visibility, it can be found that temperature, humidity and wind speed have the greatest impact. The features of the side lane and center lane in the image of expressway are more obvious by using the algorithm of de-fogging and gray processing. Then the binarization algorithm is used to extract the area and luminance ratio of the two lane lines respectively to calculate the pixel spacing of the two lane lines. The results from the two methods are roughly the same. Then the linear relationship between pixel distance and actual distance is obtained by using perspective transformation and cross-ratio invariance. Finally, the above algorithm is applied to the picture set in batches, and the change curve of expressway visibility with time is obtained. The relation between the attenuation coefficient and discrete time is obtained by using the relation curve between the visibility (MOR) and time and the visibility measure equation. Then, the relation between attenuation coefficient and continuous time is fitted by polynomial difference algorithm, and the slope change curve of the fitted curve is obtained. It is concluded that the change trend of fog is increasing or decreasing.

Keywords

Visibility, Multiple nonlinear regression model, Perspective transformation, Lminance pair ratio algorithm.

1. Introduction

1.1 Background

The video visibility detection method combines atmospheric optical analysis with image processing and artificial intelligence technology. Through the analysis and processing of the video image, the relationship between the video image and the real scene is established, and then the visibility value is calculated indirectly according to the change of image features.

However, the existing visibility detection methods based on video images are difficult to accurately estimate visibility due to the indirect calculation. In particular, most of these methods only select a small amount of video and intercept some inherent characteristics of the image [1,2], which are estimated based on Koschmieder's law [3,4], but do not make full use of the continuous information of the video, so the estimation accuracy is not high and there is a large room for improvement. This paper predicts the law of fog weather by referring to [5,6].

As a result of the general situation, visibility is 2000 meters or 3000 meters on the road traffic, almost no impact on aircraft flying, but in bad weather, especially fog conditions need to accurately estimate

the current, especially to predict the future visibility. Therefore, this project only focuses on the evolution of fog. In fact, the formation and dispersal of fog has its own laws, usually related to meteorological factors near the ground. The video contains a wealth of information, especially information about the changing process of fog. Making full use of this information can not only improve the accuracy of visibility estimation, but also predict fog dissipation.

In foggy weather, general visibility is related to meteorological observations on the ground. AMOS observed meteorological data: according to the airport station pressure (have) (HPA), high pressure landing area (QFE 06), modified sea level pressure (QNH), temperature (TEMP), relative humidity (RH), dew point temperature (DEWPOINT), 2 minutes on average wind speed (WS2A), 2 minutes on average direction (WD2A), 2 minutes on average (CW2A) and vertical wind speed airport visibility data: 1 minute on average RVR value (RVR_1A) relevant mathematics models are established.

1.2 Model assumptions

1. Visibility is only affected by meteorological observation factors on the ground and is not affected by other factors.
2. The data given are true and effective, and the visibility given is the actual visibility.
3. The visibility (RVR) corresponding to any frame of video per minute is the same, that is, the content of fog per minute does not change significantly.
4. If visibility (RVR) is missing in a certain period of time in the data set, the average value of the data existing in this period is used instead.
5. The image data given is the image of each frame in the video sequence changing according to time.
6. The camera is at the same Angle when shooting video.
7. The distance between the intermediate lines of the expressway remains unchanged.

1.3 Symbol description

Table 1 Symbol table

symbol	meaning
x_1	PAINS(HPA)
x_2	QFE 06
x_3	QNH
x_4	TEMP
x_5	RH
x_6	DEWPOINT
x_7	WS2A
x_8	WD2A
x_9	CW2A
y	RVR_1A
β	Deflection regression coefficient
s_k	The k th gray value
n_k	The number of pixels with s_k
J^c	Represents each channel of a color image
$\tilde{t}(x)$	An estimate of fluoroscopy
Cross Ratio	Cross Ratio
K	The ratio of brightness
θ	Attenuation coefficient

2. Establishment and solution of the model

2.1 A model of visibility and surface meteorological observations

2.1.1 Analysis

In foggy weather, general visibility is related to meteorological observations on the ground. In this paper, meteorological data observed at airports are used as input variables and visibility at airports as output variables. You can see that this is a function of several variables problem. In regression analysis, if there are two or more independent variables, it is called multiple regression.

In fact, a phenomenon is often associated with multiple factors, and it is more effective and practical to predict or estimate dependent variables jointly by the optimal combination of multiple independent variables than to predict or estimate only one independent variable. In this paper, multiple linear and nonlinear regression models are used to fit the relation.

2.1.2 Adopt multiple linear regression method

General pattern of multiple linear regression model:

$$y = \beta_0 + \beta_1 x_1 + \beta_2 x_2 + \dots + \beta_k x_k \quad (1)$$

β is the partial regression coefficient. The coefficient estimation in the multiple linear regression model is the same as that in the unitary linear regression model, which is to find the sum of squares of errors. Generally, the least square method is used to solve the coefficient.

Visibility is an important factor in meteorological observation and also reflects atmospheric transparency, which is a very important indicator. In view of the poor accuracy of the existing visibility detection methods and the high cost of installing large quantities of detection instruments, a visibility detection model based on multiple regression was proposed. First, meteorological and visibility data observed by AMOS at the airport were processed. Then, the least square method is used to train the multiple regression model of the characteristics and visibility. Finally, the residual graph and R square are used for verification.

In data processing, we will take the method of one data per minute to first take the average of the data per minute in WS2A, WD2A, CW2A and RVR_1A, and finally put the 9 independent variables and one dependent variable into a TXT text and named in English to facilitate MATLAB reading. After processing, each of the 10 variables has 1440 sets of data in corresponding time period. After establishing a multiple regression model in MATLAB and reading the variable data in TXT, the following residual figure can be obtained:

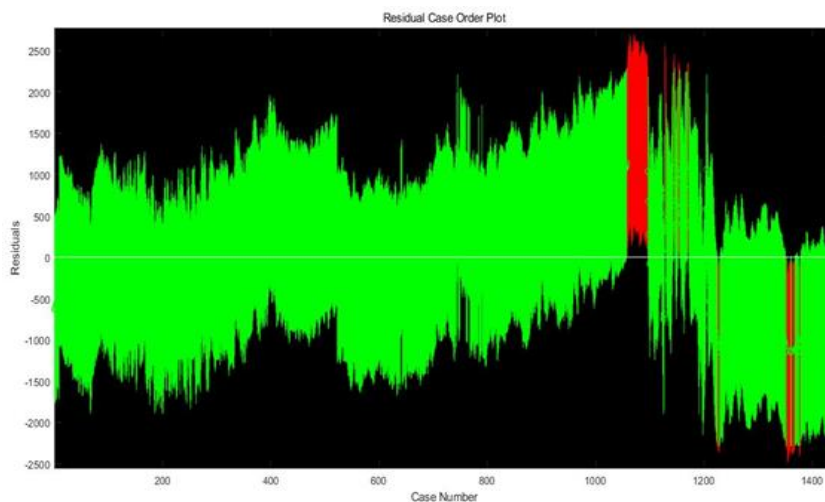


Fig.1 residual

By studying the figure above, we find that 67 out of 1440 points are outliers, and all of these outliers fall outside the confidence interval. It can be found from the residual graph that the multiple linear

regression model basically includes the influence of nine meteorological observation data on visibility, but the error is relatively large.

Establishing the regression model in MATLAB and reading the specific data can obtain 10 regression coefficients of deflection β_i :

Table 2 Regression coefficient table

coefficient	β_0	β_1	β_2	β_3	β_4	β_5	β_6	β_7	β_8	β_9
value	-259681	0	50916	-50562	-831	-212	1009.5	-197	-0.4	-103
R2=0.67										

Thus, the specific relationship between meteorological observation data and airport visibility can be obtained:

$$y = -2.6 * 10^5 + 5100x_2 - 5100x_3 - 830x_4 - 210x_5 + 1010x_6 - 200x_7 - 100x_9 \quad (2)$$

However, it can be seen from the above table that after the linear regression was fitted by MATLAB, the R squared value obtained was 0.67, so the fitting effect was not very good and needed further processing.

2.1.3 Multiple nonlinear regression method is adopted

In order to find out the influence of complex meteorological factors on visibility variation, the multivariate nonlinear regression relationship between meteorological factors and visibility was established by using AMOS ground meteorological observation data at the airport.

This paper USES Python to fit the multiple nonlinear regression model. After Python fitting, the specific relationship between ground meteorological observation factors and airport visibility can be obtained as follows:

$$y = \beta_1x_1 + \dots + \beta_9x_9 + \beta_{10}x_1x_2 + \dots + \beta_{18}x_1x_9 + \beta_{19}x_2x_3 + \dots + \beta_ix_8x_9 + \beta_{i+1}x_1x_2^2 + \dots + \beta_jx_8x_9^2 + \beta_{j+1}x_1^3 + \dots + \beta_{220}x_9^3 \quad (3)$$

Among them, is the regression coefficient, and there are 220 regression coefficients in this specific relationship.

After using MATLAB to establish the multiple linear regression model and Python to establish the multiple nonlinear regression model, we can find that the specific relations of ground meteorological observation conditions and airport visibility obtained by the two models are very different. Therefore, on this basis, Python is used to detect the error values of the multiple linear regression model and the multiple nonlinear regression model respectively. Among them, 1440 is used for 70 percent of the data for training and 30 percent for testing, and the following variance diagram can be obtained:

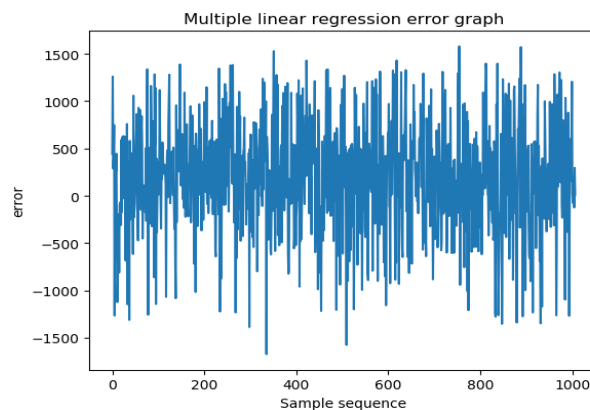


Fig. 2 Multiple linear regression training error graph

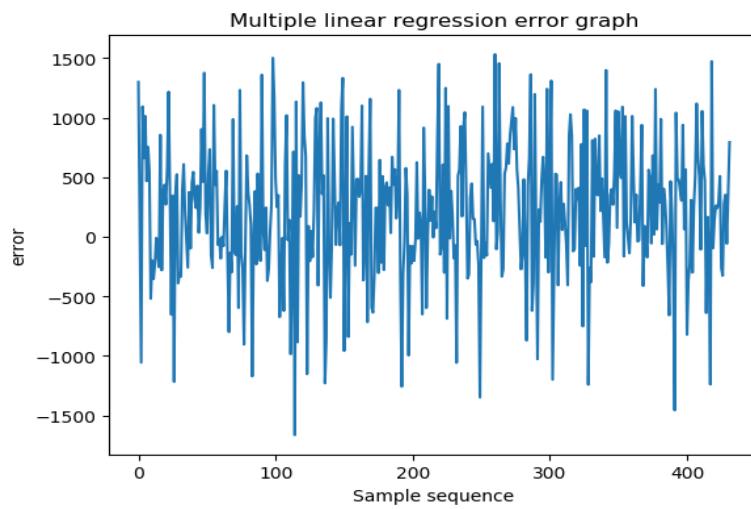


Fig.3 Multiple linear regression test error graph

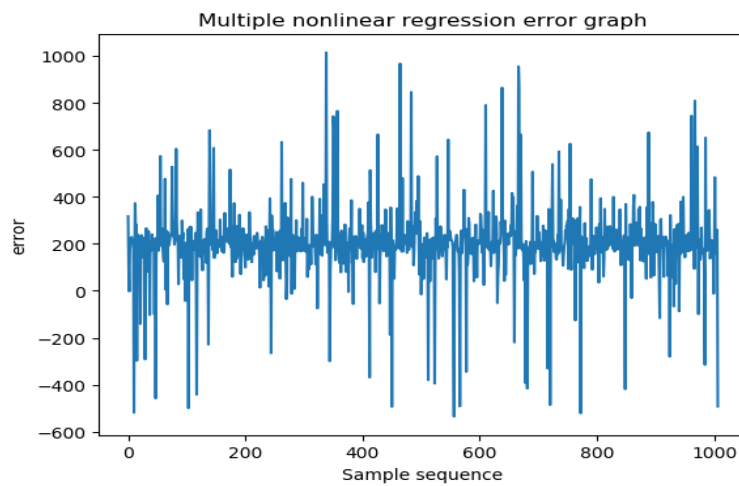


Fig .4 Multiple nonlinear regression training error

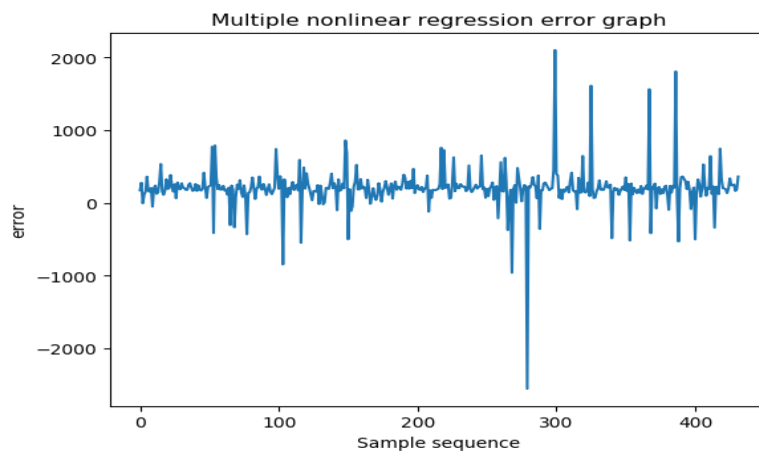


Fig.5 Error Diagram of Multiple Nonlinear Regression

It can be found from the above four error graphs that the multiple nonlinear regression error is relatively small, and the number of outliers is also less than the multiple linear regression. Therefore, the multiple nonlinear regression model is more effective in finding the relationship between meteorological factors and airport visibility.

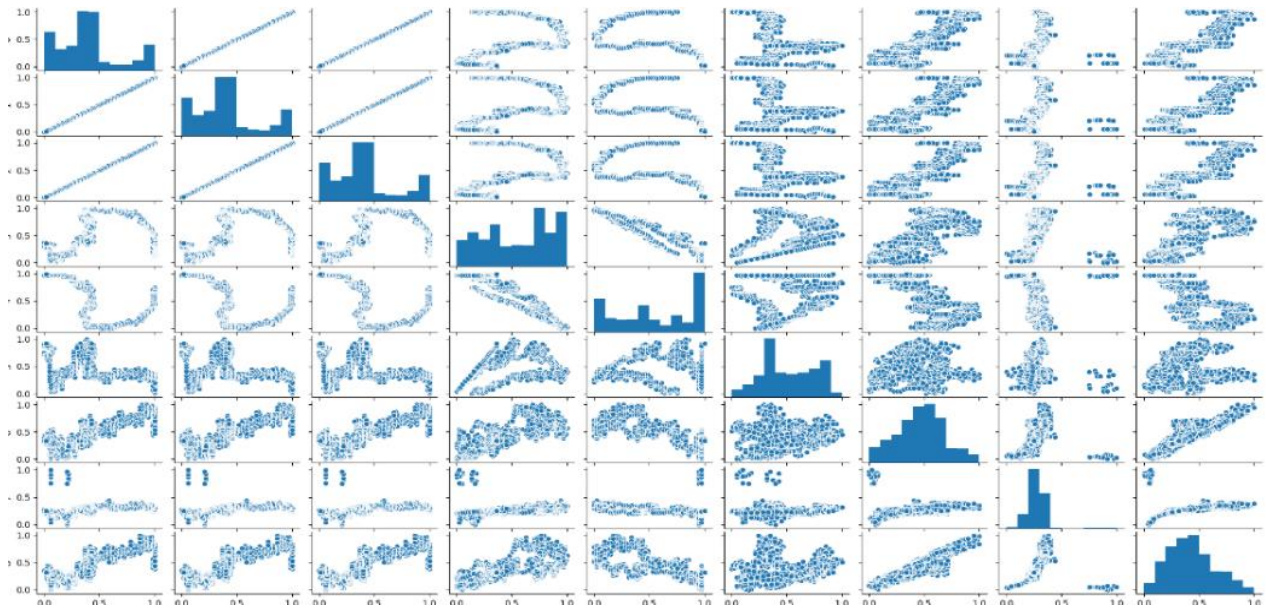


Fig.6 Correlation diagram

The correlation between meteorological observation factors and visibility can be obtained by studying the figure above. Each column in the figure above represents the correlation between an independent variable and visibility, where the correlation greater than 0.8 needs to be eliminated, otherwise a large number of outliers will occur.

2.2 Visibility modeling

2.2.1 Analysis

In this model, the grayscale value and brightness difference of objects under different depth of field are used to extract the most prominent feature of freeway - side lane and road center line. The two methods extract the recognisable side lane line based on the length of pixel position and the pixel-based distance between the road center line respectively.

By using the perspective transform method (keyhole imaging) and the constant feature of the projection intersection ratio, the actual scale of the image was demarcated to find the linear relationship between the lane divider and the middle line of the road. For the image, because the image fog is very thick, the extraction effect of the connected area of image binarization and the brightness extraction of the side lane line is poor. Therefore, the use of the image defogging image processing algorithm makes the features to be extracted more significant.

2.2.2 Data processing

2.2.2.1 Image defogging pretreatment

(1) Dark channel prior

Normal images will have at least one color channel with a very low value, defined as a dark channel. Can be expressed as follows:

$$J^{dark}(x) = \min_{y \in \Omega(x)} (\min_{c \in \{r,g,b\}} J^c(y)) \tag{4}$$

J^c represents each channel of the color image, $\Omega(x)$ represents a window centered on pixel X.

The dark Channel priori theory points out that:

$$J^{dark} \rightarrow 0$$

In real life, there are three main factors that cause the low channel value in the dark primary color: a) shadows or projections of various objects; b) brightly coloured objects or surfaces c) darker objects or surfaces, where the image of the object is always of a dark primary colour.

The fog map formation model described by the following equation is widely used

$$I(x) = J(x)t(x) + A(1-t(x)) \quad (5)$$

In the equation, $I(x)$ is the image we have now (the image to be fog-free), $J(x)$ is the fog-free image we want to restore, A is the global atmospheric light component, $t(x)$ is transmittance

Become:

$$\frac{I^C(x)}{A^C} = t(x) \frac{J^C(x)}{A^C} + 1 - t(x) \quad (6)$$

The superscript C represents the three channels of R/G/B.

Let's first assume that transmittance $t(x)$ is constant in each window, defining as $\tilde{t}(x)$, and the value of A has been given. Then, calculate the minimum value of both sides of Equation (6) twice to get the following formula:

$$\min_{y \in \Omega(x)} \left(\min_C \frac{I^C(y)}{A^C} \right) = \tilde{t}(x) \min_{y \in \Omega(x)} \left(\min_C \frac{J^C(y)}{A^C} \right) + 1 - \tilde{t}(x) \quad (7)$$

In the above equation, J is the fog-free image to be obtained. According to the aforementioned dark channel prior theory, J is:

$$J^{dark}(x) = \min_{y \in \Omega(x)} \left(\min_C J^C(y) \right) = 0 \quad (8)$$

Therefore, it can be deduced that:

$$\min_{y \in \Omega(x)} \left(\min_C \frac{J^C(y)}{A^C} \right) = 0 \quad (9)$$

Equation (9) is substituted into Equation (7) to obtain the estimated transmittance:

$$\tilde{t}(x) = 1 - \min_{y \in \Omega(x)} \left(\min_C \frac{I^C(y)}{A^C} \right) \quad (10)$$

The presence of fog makes people feel the existence of depth of field. Therefore, it is necessary to retain a certain degree of fog when defogging. A factor between $[0,1]$ is introduced, and equation (8) becomes:

$$\tilde{t}(x) = 1 - \omega \min_{y \in \Omega(x)} \left(\min_C \frac{I^C(y)}{A^C} \right) \quad (11)$$

The final recovery formula is as follows:

$$J(x) = \frac{I(x) - A}{\max(t(x), t_0)} + A \quad (12)$$

The defogging effect is shown in the figure below:



Fig.7 Original image



Fig.8 Image after defogging

Obviously, the defogging algorithm can highlight the characteristics of lane rope and road center line, which is very helpful for feature extraction.

2.2.2.2 Binarization and brightness feature extraction

(1) Feature length extraction of binarization region contour

Gray-scale image is a three-channel RGB image fused according to a certain proportion, which can further represent the contour features to be extracted. The threshold value [27,255] is used for binarization, and the effect diagram is as follows, which can obviously extract the pixel-based distance between the side rope and the center rope in bulk.



Fig.9 Gray image after fog removal



Fig.10 Binarization image after fog removal

Table 3 The pixel length of the side lane extracted by binarization

number	The pixel length of the side lane for each image									
1-10	245	252	253	250	261	275	289	283	276	250
11-20	244	245	242	269	284	268	274	270	245	270
21-30	26	273	286	286	286	279	277	266	269	268
31-40	264	282	280	274	263	276	262	267	248	257
41-50	261	247	241	264	242	251	241	272	245	263
51-60	263	267	250	265	260	262	259	268	277	255
61-70	276	276	278	256	276	254	268	255	267	247
71-80	269	258	264	263	284	265	274	263	255	267
81-90	267	251	269	262	264	249	261	243	252	267
91-100	253	258	245	259	261	245	249	259	262	252

(2) Extract feature length according to brightness difference

Binary region extraction can be very simple to extract feature length, but there is a problem of region missing affecting the accuracy of results, so the use of brightness difference can be used to estimate visibility. According to (1), two-point coordinates A(720,483) and B (568,417) on the left lane line are shown in the figure below:

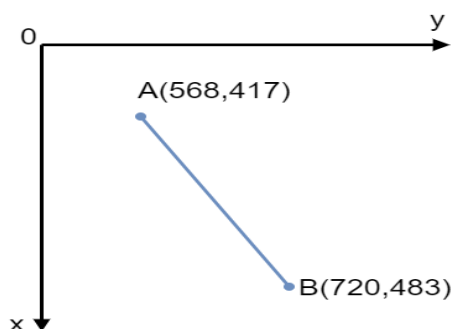


Fig.11 Left lane line in the image coordinate system

The linear fitting method can be used to determine the lines that need to extract brightness.

$$x = k(y - y_a) + x_a \quad (13)$$

From A to B we get k is equal to 0.434.become:

$$x = 0.434(y - 720) + 483 \quad (14)$$

After image gray processing, all brightness values on the whole line can be obtained. A bright object is clearly visible against a bright background, or a bright object is clearly visible against a dark background. An indicator of this difference is the logarithm of brightness K . Set B_0 as the intrinsic brightness of the target object and B'_0 as the intrinsic brightness of the background, then the cross-ratio of the luminance is defined as:

When $B'_0 \geq B_0$

$$K = \frac{|B'_0 - B_0|}{B'_0} \quad (15)$$

When $B'_0 < B_0$

$$K = \frac{|B'_0 - B_0|}{B_0} \quad (16)$$

When $K \geq 0.05$, objects are clearly visible. When the conditions are met, the side lane line can be seen. If the conditions are not met, the pixel position is recorded, and then the pixel distance between the starting pixel coordinates (720,483) and the ending pixel is calculated, which is denoted as the visibility pixel distance.

The following data are obtained:

Table 4 The pixel length of the side lane extracted by the luminance to the ratio

number	The pixel length of the side lane for each image									
1—10	254	255	258	247	235	258	260	257	261	262
11—20	241	247	237	226	259	247	243	258	260	264
21—30	264	162	247	259	235	201	247	270	243	209
31—40	256	264	256	264	263	273	282	281	282	282
41—50	282	273	255	256	259	264	238	283	281	280
51—60	262	272	247	162	244	262	245	244	260	249
61—70	263	241	247	264	249	237	264	264	264	263
71—80	274	247	264	264	264	243	264	264	243	257
81—90	241	261	264	257	259	262	250	278	276	276
91—100	276	264	243	243	221	235	243	256	275	100

2.2.3 Image scale calibration based on perspective transformation method

2.2.3.1. Cross-ratio invariance of camera imaging

According to the principle of pinhole imaging, when points in 3d space are projected onto a specific projective plane, parallel lines in 3D space will intersect at a projective point on the projective plane, which is the vanishing point in the projective plane. The vanishing point on the projective plane corresponds to infinity in three dimensions which is the end of the horizon. The vanishing point is only related to the direction of the line, and a vanishing point in the projective plane can be determined by a set of parallel lines in three-dimensional space. A collinear point of extinction determined by a group of parallel lines on a plane is called the extinction line (horizon line).

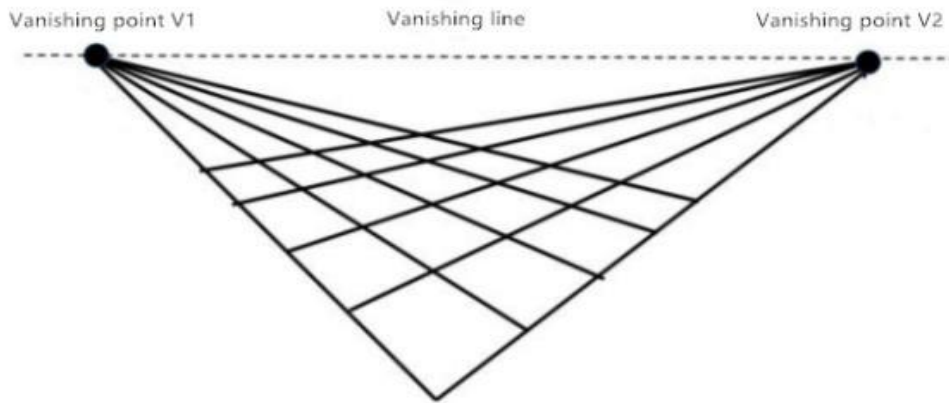


Fig. 12 Projection of 3D image

According to the properties of projective transformation and perspective projection, the intersection ratio of the four collinear points in the image is equal to that in the real world. Therefore, the distance information in the image can be determined by the invariance of the cross ratio.

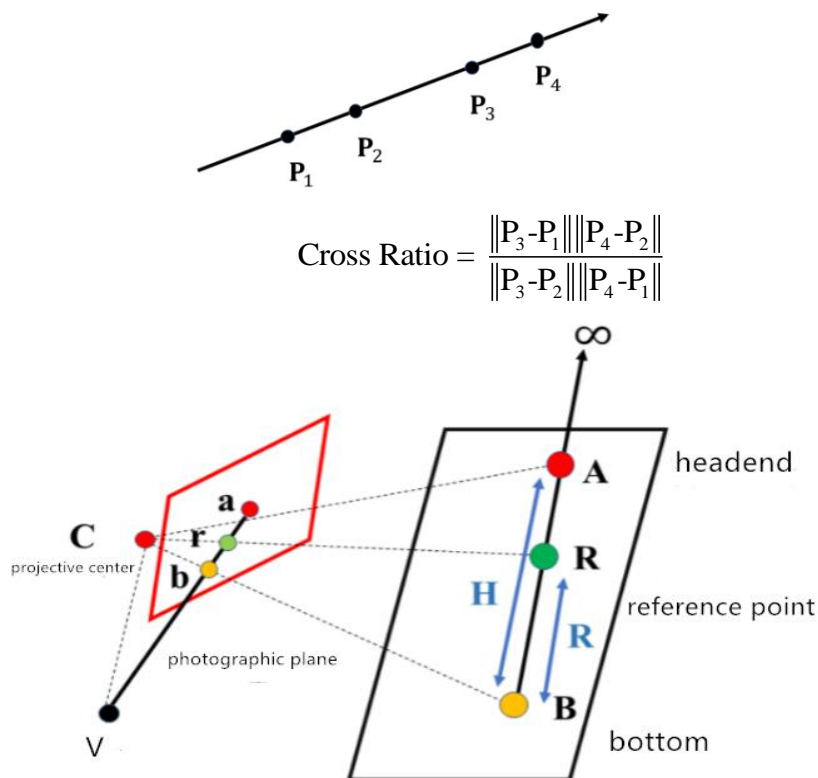


Fig. 13 3d projection

$$\text{Cross Ratio} = \frac{\|A-B\| \|\infty-R\|}{\|R-B\| \|\infty-A\|} = \frac{H}{R} \tag{18}$$

$$\text{Cross Ratio} = \frac{\|a-b\| \|v_z-r\|}{\|r-b\| \|v_z-a\|} = \frac{H}{R} \tag{19}$$

Therefore, according to the invariance of the gross ratio, the length and distance of the object can be solved by solving the vanishing point in the image. This problem can be constructed as follows.

2.2.3.2. Model construction for solving actual distance

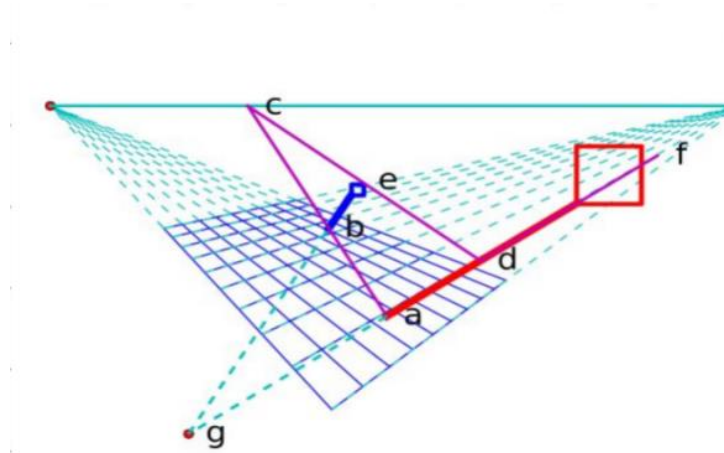


Fig. 14 3d simulation projection

The line segment from the point on the horizon to any two points is parallel to each other, the projection of be onto ad, and the extension of be intersects ad at infinity at g. Line segments be, ed, da and ab form rectangles in real space. On online gf, it can be known from the cross-ratio invariance that:

$$\frac{AD}{AF} / \frac{GD}{GF} = \frac{ad}{af} / \frac{gd}{gf} \tag{20}$$

The upper case letters represent the actual distance, and the lower case letters represent the distance measured directly on the graph.

For this problem, a mapping model can be constructed:

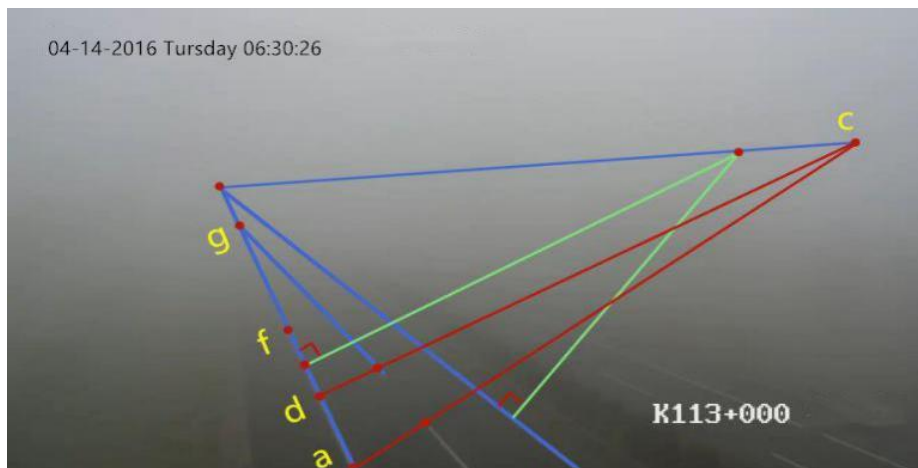


Fig. 15 3d projection of the actual highway

The ratio of image length L to actual image pixel size L is:

$$\lambda = \frac{L}{l} = 3.345 \tag{21}$$

$\frac{GD}{GF} \approx 1$, AD is the distance between the center lane of the expressway, we can Obtained:

$$AF = Kaf, K = 47.79\lambda \tag{22}$$

The actual visibility can be changed to:

Table 5 Actual visibility table

number	The actual visibility of each image/m									
1-10	40.6	40.8	41.3	39.6	37.7	41.3	41.7	41.1	41.8	42
11-20	38.5	39.6	38	36.2	41.5	39.6	38.9	41.3	41.7	42.3
21-30	42.3	26	39.6	41.5	37.7	32.2	39.6	43.2	38.9	33.4
31-40	41	42.3	41	42.3	42.1	43.7	45.1	45	45.1	45.1
41-50	45.1	43.7	40.8	41	41.5	42.3	38.1	45.3	45	44.8
51-60	42	43.6	39.6	26	39	42	39.2	39	41.7	39.9
61-70	42.2	38.7	39.6	42.3	39.9	38	42.3	42.3	42.3	42.2
71-80	43.9	39.6	42.3	42.3	42.3	38.9	42.3	42.3	38.9	41.1
81-90	38.7	41.8	42.3	41.1	41.5	42	40.1	44.5	44.2	44.2
91-100	44.2	42.3	38.9	38.9	35.3	37.7	38.9	41	44.1	16

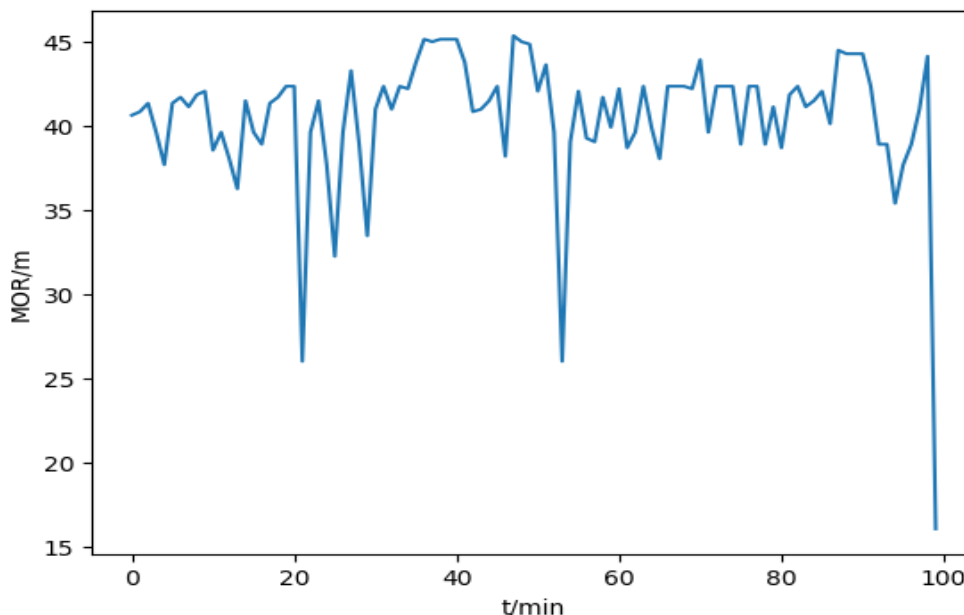


Fig. 16 Variation of visibility MOR over time

2.3 Forecast the trend of fog change

2.3.1 Analysis

Trends on the strength of the fog and close relationship, such as air temperature, wind direction, air pressure, visibility has got the above change with the time, can use the basic equation of visibility measurement model, get the curve of the fog concentration change with time, and then using 10 order polynomial fitting method, indirect get fog over time trends, then slope method is used to estimate how fast the change trend of the heavy fog.

2.3.2 Establishment of model

Basic equation of visibility measurement:

$$F = F_0 e^{-\sigma z} \tag{23}$$

F and F0 respectively represent the observed and incident light intensity. Parameter σ is called attenuation coefficient. The larger σ is, the thicker the fog is. This formula can be obtained as follows:

$$MOR = \frac{\log(F / F_0)}{-\sigma} = \frac{\log(0.05)}{-\sigma} \tag{24}$$

Become:

$$\sigma = -\frac{\log(0.05)}{MOR} \tag{25}$$

The average MOR per minute that can be known from the third digit.

The tenth degree polynomial model is constructed

$$\sigma(t) = \omega_0 + \omega_1 t + \omega_2 t^2 + \omega_3 t^3 + \dots + \omega_{10} t^{10} \tag{26}$$

The weights obtained are shown in the following table:

Table 6 Weight parameters table

ω	ω_0	ω_1	ω_2	ω_3	ω_4	ω_5
	1.16e-17	-4.9e-15	8.9e-13	-8.5e-11	4.6e-9	-1.4e-7
ω	ω_6	ω_7	ω_8	ω_9	ω_{10}	
	2.2e-6	-1.5e-5	3.5e-5	-9.2e-7	7.4e-2	

Draw the fitting curve and its derivative:

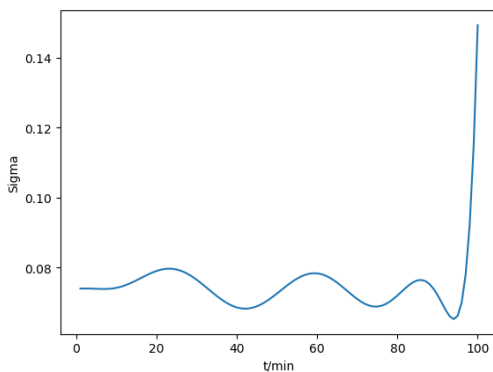


Fig.17 Change of σ over time

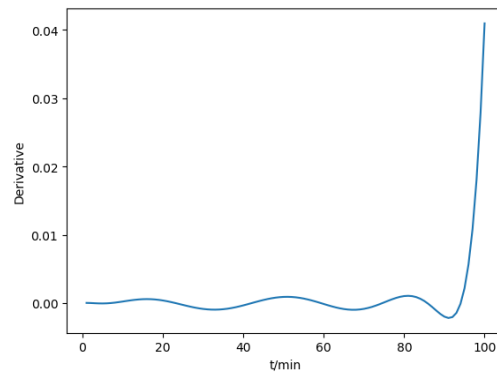


Fig.18 Derivative graph of σ over time

As you can see from the picture:

Within 0-20min, σ gradually increases and the fog becomes more and more dense; within 20-40min, σ gradually decreases and the fog gradually reduces to the minimum value; within 40-60min, it gradually increases and then decreases within 60-75min. and then reaches the peak value at 90min. It has obvious periodic component, which is about 40min. The data after 90min can be ignored due to the existence of polynomial fitting error. The derivative of σ has little change and is relatively stable, so it can be concluded that fog does not dissipate or grow too fast.

References

- [1] S. K. Nayar, S. G. Narasimhan, Vision in bad weather, ICCV'99.
- [2] R. T. Tan, Visibility in bad weather from a single image, CVPR, 2008.
- [3] N. Hautiere, J-P Tarel, J Lavenant D. Aubert, Automatic fog detection and estimation of visibility distance through use of onboard camera, Machine Vision and Application, 2006, 17(1):8-20.
- [4] C.Sakaridis,D.Dai,L.V.Gool,Semantic foggy scene understanding with synthetic data, International J. Computer Vision, 2018, 3.
- [5] Criminisi A, Reid I, Zisserman A. Single view metrology[J]. International Journal of Computer Vision, 2000, 40(2):123-148.
- [6] Hartley R, Zisserman A. Multiple view geometry in computer vision[M]. Cambridge university press, 2003.